Supplemental Information of

Evolution of ^{231}Pa and ^{230}Th in overflow waters of the North Atlantic

Feifei Deng et al.

Correspondence to: Feifei Deng (feifei.deng@earth.ox.ac.uk)

S1. Data of water-column ^{231}Pa, ^{230}Th and ^{232}Th concentrations, and ^{231}Pa/^{230}Th ratios along GEOVIDE section and details of correction

Table S1 Water-column ^{231}Pa, ^{230}Th and ^{232}Th concentrations, and ^{231}Pa/^{230}Th ratios along GEOVIDE section

Station	Depth	^{231}Pa	^{231}Pa	^{231}Pa$_{corr}$	2se	^{230}Th	^{230}Th	^{230}Th$_{corr}$	2se	^{232}Th	^{232}Th	2se	^{231}Pa/^{230}Th	2se
	m	fg/kg	dpm/1000l	dpm/1000		fg/kg	dpm/1000l	dpm/1000l		pg/kg	dpm/1000l			
1	3445.3	2.270	0.244	0.244	0.011									
40.33°N	2955.3	2.465	0.265	0.265	0.013									
10.04°W	2465.8	1.988	0.214	0.213	0.013	9.077	0.425	0.415	0.012	52.33	0.01306	0.00027	0.513	0.035
	1974.9	1.592	0.171	0.171	0.012	5.716	0.267	0.260	0.010	43.47	0.01084	0.00021	0.657	0.053
	1385.3	1.522	0.164	0.163	0.014	3.507	0.164	0.156	0.009	44.96	0.01122	0.00024	1.044	0.106
	1039.6	1.176	0.126	0.126	0.012	3.556	0.166	0.156	0.013	59.80	0.01492	0.00028	0.806	0.102
	495.6	0.861	0.093	0.092	0.013	3.744	0.175	0.162	0.010	72.77	0.01815	0.00034	0.564	0.089
	246.9	0.635	0.068	0.067	0.011	2.867	0.134	0.117	0.009	99.60	0.02485	0.00057	0.575	0.103
	49.6	0.641	0.069	0.067	0.012	2.917	0.136	0.107	0.011	171.16	0.04270	0.00078	0.628	0.133
	4.7	0.238	0.026	0.023	0.005	4.006	0.187	0.143	0.006	255.90	0.06384	0.00108	0.158	0.033
13	5330.4	2.093	0.225	0.202	0.015	8.823	0.413	0.411	0.009	22.79	0.00568	0.00010	0.491	0.038
41.38°N	5263.1	2.421	0.260	0.234	0.016	12.790	0.598	0.595	0.011	33.12	0.00826	0.00013	0.393	0.028
13.89°W	5194.3	2.751	0.296	0.295	0.015	15.923	0.745	0.738	0.020	39.61	0.00988	0.00019	0.400	0.022
	4903.9	2.013	0.216	0.216	0.009	14.920	0.698	0.692	0.017	35.27	0.00880	0.00018	0.312	0.015
	4417.8	2.627	0.282	0.282	0.015	11.285	0.528	0.523	0.015	28.70	0.00716	0.00015	0.539	0.032
	3444	2.399	0.258	0.258	0.009	8.276	0.387	0.383	0.011	22.33	0.00557	0.00013	0.672	0.030
	2464.7	1.569	0.169	0.168	0.016	5.894	0.276	0.270	0.012	30.57	0.00763	0.00016	0.622	0.065
	1187.3	0.869	0.093	0.093	0.007	3.369	0.158	0.151	0.010	37.16	0.00927	0.00019	0.616	0.062
	989.1	1.239	0.133	0.133	0.009	4.284	0.200	0.193	0.011	41.38	0.01032	0.00021	0.686	0.061
	248.4	0.602	0.065	0.065	0.007									
	148.5	0.525	0.056	0.056	0.008									
	29.7	0.508	0.055	0.055	0.007	0.570	0.027	0.026	0.009	5.60	0.00140	0.00009	2.122	0.808
	4.3	0.330	0.036	0.035	0.005	0.403	0.019	0.018	0.009	6.70	0.00167	0.00008	2.004	1.003

Station	Depth	^{231}Pa	^{231}Pa	$^{231}Pa_{corr}$	2se	^{230}Th	^{230}Th	$^{230}Th_{corr}$	2se	^{232}Th	^{232}Th	2se	$^{231}Pa/^{230}Th$	2se
	m	fg/kg	dpm/1000l	dpm/1000		fg/kg	dpm/1000l	dpm/1000l		pg/kg	dpm/1000l			
21	4514.9	2.605	0.280	0.280	0.009	6.223	0.291	0.287	0.012	20.99	0.00524	0.00010	0.973	0.051
46.54°N	4475	2.404	0.258	0.258	0.011	6.338	0.296	0.292	0.017	25.11	0.00627	0.00015	0.883	0.064
19.67°W	4426.3	2.413	0.259	0.259	0.011	5.889	0.275	0.272	0.009	19.57	0.00488	0.00010	0.952	0.050
	4279.6	2.497	0.268	0.268	0.011	6.042	0.283	0.279	0.012	20.48	0.00511	0.00011	0.961	0.058
	3929.3	2.081	0.224	0.223	0.010	5.598	0.262	0.258	0.010	20.11	0.00502	0.00009	0.865	0.051
	3443.3	1.930	0.207	0.207	0.013	4.755	0.222	0.219	0.008	18.16	0.00453	0.00009	0.945	0.068
	2268.9	1.114	0.120	0.120	0.013	5.287	0.247	0.242	0.011	30.49	0.00761	0.00012	0.495	0.059
	1482.7	0.995	0.107	0.107	0.007	2.607	0.122	0.117	0.009	26.83	0.00669	0.00009	0.910	0.090
	788.4	0.873	0.094	0.094	0.008	1.438	0.067	0.063	0.010	25.41	0.00634	0.00011	1.489	0.267
	445.5	0.679	0.073	0.073	0.009	2.309	0.108	0.101	0.009	39.91	0.00996	0.00014	0.719	0.107
	246.9	0.595	0.064	0.064	0.007	1.770	0.083	0.077	0.008	33.41	0.00833	0.00011	0.827	0.125
	98.1	0.607	0.065	0.065	0.009	1.445	0.068	0.063	0.007	28.01	0.00699	0.00011	1.034	0.184
	13.9	0.536	0.058	0.057	0.009	0.316	0.015	0.013	0.008	10.81	0.00270	0.00009	4.439	3.008
	3.7	0.522	0.056	0.056	0.008	0.110	0.005	0.004	0.008	7.95	0.00198	0.00008	14.851	30.841
26	4116.3	1.162	0.125	0.124	0.011	3.551	0.166	0.159	0.010	42.15	0.01052	0.00020	0.783	0.084
50.28°N	2758.5	0.813	0.087	0.087	0.009	3.162	0.148	0.138	0.008	57.40	0.01432	0.00027	0.629	0.078
22.60°W	1973.5	0.745	0.080	0.079	0.008	2.952	0.138	0.128	0.010	56.40	0.01407	0.00026	0.620	0.078
	989.1	0.695	0.075	0.075	0.007									
	296.7	0.503	0.054	0.054	0.006									
	74.4	0.408	0.044	0.044	0.007	0.792	0.037	0.035	0.011	13.57	0.00339	0.00010	1.261	0.441

Station	Depth	^{231}Pa	^{231}Pa	$^{231}Pa_{corr}$	2se	^{230}Th	^{230}Th	$^{230}Th_{corr}$	2se	^{232}Th	^{232}Th	2se	$^{231}Pa/^{230}Th$	2se
	m	fg/kg	dpm/1000l	dpm/1000		fg/kg	dpm/1000l	dpm/1000l		pg/kg	dpm/1000l			
32	3218.7	0.973	0.105	0.104	0.009	5.617	0.263	0.255	0.009	43.48	0.01085	0.00013	0.408	0.038
55.51°N	3218.5	0.984	0.106	0.106	0.008	1.803	0.084	0.082	0.008	15.25	0.00381	0.00009	1.292	0.163
26.71°W	3049.9	1.131	0.122	0.121	0.007	3.399	0.159	0.155	0.008	20.44	0.00510	0.00009	0.780	0.059
	2949.6	1.076	0.116	0.116	0.011	1.866	0.087	0.085	0.008	12.96	0.00323	0.00008	1.359	0.179
	2854.3	1.004	0.108	0.108	0.012	2.775	0.130	0.127	0.011	16.46	0.00411	0.00009	0.848	0.120
	2610.4	1.109	0.119	0.119	0.008	1.947	0.091	0.089	0.009	12.01	0.00300	0.00009	1.338	0.161
	2218.8	0.843	0.091	0.090	0.009	1.426	0.067	0.065	0.008	11.46	0.00286	0.00009	1.398	0.224
	1676.9	1.200	0.129	0.129	0.008	1.000	0.047	0.045	0.008	9.00	0.00225	0.00008	2.848	0.512
	1185.5	1.087	0.117	0.116	0.008	3.708	0.173	0.166	0.009	40.46	0.01010	0.00013	0.699	0.064
	890.5	0.872	0.094	0.093	0.009	1.768	0.083	0.078	0.008	29.00	0.00724	0.00010	1.202	0.168
	445.3	0.944	0.101	0.101	0.009	3.038	0.142	0.134	0.009	46.20	0.01152	0.00015	0.753	0.081
	222.9	0.568	0.061	0.061	0.008	1.827	0.085	0.079	0.008	39.69	0.00990	0.00013	0.772	0.124
	98.9	0.553	0.059	0.059	0.015	6.777	0.317	0.312	0.010	27.70	0.00691	0.00010	0.189	0.049
	29.5	0.613	0.066	0.066	0.017	5.628	0.263	0.258	0.010	27.73	0.00692	0.00011	0.254	0.066
	5.8	0.584	0.063	0.063	0.009	0.159	0.007	0.006	0.010	9.92	0.00247	0.00009	10.990	18.598
38	1338.1	1.604	0.172	0.172	0.013	1.723	0.081	0.078	0.009	16.07	0.00401	0.00011	2.214	0.308
58.84°N	1303.6	1.336	0.144	0.143	0.006	3.440	0.161	0.156	0.012	29.18	0.00728	0.00015	0.919	0.084
31.27°W	1234.5	1.088	0.117	0.117	0.007	3.521	0.165	0.160	0.009	28.39	0.00708	0.00015	0.730	0.061
	1084	0.863	0.093	0.092	0.006	3.738	0.175	0.169	0.011	31.67	0.00790	0.00016	0.546	0.051
	494.2	1.621	0.174	0.174	0.015	3.256	0.152	0.145	0.010	39.87	0.00995	0.00019	1.195	0.133
	198.4	1.258	0.135	0.135	0.008	3.217	0.150	0.142	0.008	46.64	0.01164	0.00022	0.946	0.078
	108.7	1.274	0.137	0.136	0.012	2.883	0.135	0.127	0.008	42.89	0.01070	0.00021	1.071	0.117
	20.3	0.836	0.090	0.090	0.008	0.940	0.044	0.042	0.008	11.88	0.00296	0.00009	2.143	0.463
	5.3	1.230	0.132	0.132	0.015	0.895	0.042	0.040	0.009	11.59	0.00289	0.00009	3.314	0.856

Station	Depth	^{231}Pa	^{231}Pa	$^{231}Pa_{corr}$	2se	^{230}Th	^{230}Th	$^{230}Th_{corr}$	2se	^{232}Th	^{232}Th	2se	$^{231}Pa/^{230}Th$	2se
	m	fg/kg	dpm/1000l	dpm/1000		fg/kg	dpm/1000l	dpm/1000l		pg/kg	dpm/1000l			
44	2918.9	0.839	0.090	0.090	0.010	2.492	0.117	0.113	0.008	22.85	0.00570	0.00013	0.799	0.107
59.62°N	2878.5	0.875	0.094	0.094	0.009	2.591	0.121	0.117	0.009	24.44	0.00610	0.00013	0.802	0.097
38.95°W	2829	0.723	0.078	0.078	0.013									
	2681.9	0.651	0.070	0.070	0.015	2.746	0.128	0.124	0.009	25.27	0.00630	0.00014	0.562	0.124
	2561	1.164	0.125	0.125	0.014	4.964	0.232	0.228	0.011	26.47	0.00660	0.00015	0.548	0.067
	2216.6	0.910	0.098	0.097	0.016	6.275	0.294	0.288	0.011	31.25	0.00780	0.00016	0.338	0.057
	1776	1.416	0.152	0.152	0.024	5.967	0.279	0.272	0.009	39.66	0.00990	0.00019	0.557	0.089
	1382.5	1.186	0.127	0.127	0.017	5.941	0.278	0.271	0.009	41.00	0.01023	0.00020	0.469	0.064
	1087.5	0.795	0.085	0.085	0.011	3.925	0.184	0.176	0.009	40.73	0.01016	0.00019	0.481	0.069
	593.2	1.116	0.120	0.119	0.022	4.372	0.204	0.196	0.010	46.81	0.01168	0.00022	0.608	0.116
	297.3	1.083	0.116	0.116	0.012	4.195	0.196	0.189	0.013	42.29	0.01055	0.00021	0.614	0.079
	78.8	0.929	0.100	0.099	0.011	3.534	0.165	0.158	0.009	39.69	0.00990	0.00019	0.628	0.080
	25.5	0.998	0.107	0.107	0.010	1.465	0.069	0.066	0.009	16.50	0.00412	0.00011	1.631	0.267
	5.5	0.722	0.078	0.077	0.020	1.408	0.066	0.063	0.007	14.99	0.00374	0.00010	1.224	0.351
60	1710.9	0.844	0.091	0.090	0.004	3.861	0.181	0.175	0.010	31.42	0.00784	0.00018	0.516	0.037
59.80°N	1652.6	0.881	0.095	0.094	0.004	4.118	0.193	0.187	0.010	33.28	0.00830	0.00018	0.505	0.035
42.01°W	1603.1	0.845	0.091	0.090	0.005	4.186	0.196	0.190	0.015	33.74	0.00842	0.00019	0.476	0.044
	1481.2	0.813	0.087	0.087	0.004	4.278	0.200	0.194	0.010	33.94	0.00847	0.00019	0.448	0.033
	989.7	1.087	0.117	0.116	0.005	5.379	0.252	0.244	0.012	45.60	0.01138	0.00023	0.477	0.031
	495.5	0.911	0.098	0.097	0.010	3.782	0.177	0.170	0.008	39.63	0.00989	0.00019	0.573	0.063
	247.9	0.851	0.091	0.091	0.014	3.252	0.152	0.145	0.009	40.61	0.01013	0.00020	0.628	0.106
	99.1	0.826	0.089	0.088	0.012	2.431	0.114	0.108	0.008	34.75	0.00867	0.00017	0.821	0.129
	19.5	0.887	0.095	0.095	0.019	1.455	0.068	0.065	0.010	18.14	0.00452	0.00012	1.465	0.372
	3.7	0.829	0.089	0.089	0.015	1.626	0.076	0.072	0.008	22.32	0.00557	0.00013	1.231	0.247

Station	Depth	^{231}Pa	^{231}Pa	^{231}Pa$_{corr}$	2se	^{230}Th	^{230}Th	^{230}Th$_{corr}$	2se	^{232}Th	^{232}Th	2se	^{231}Pa/^{230}Th	2se
	m	fg/kg	dpm/1000l	dpm/1000		fg/kg	dpm/1000l	dpm/1000l		pg/kg	dpm/1000l			
64	2466.8	0.759	0.082	0.081	0.012	3.310	0.155	0.150	0.009	25.71	0.00641	0.00014	0.541	0.085
59.067°N	2423.6	0.828	0.089	0.089	0.012	3.780	0.177	0.172	0.011	26.12	0.00652	0.00016	0.515	0.079
46.08°W	2374	0.958	0.103	0.103	0.012	3.835	0.179	0.175	0.008	27.16	0.00678	0.00015	0.588	0.073
	2226.6	1.051	0.113	0.113	0.017	5.407	0.253	0.248	0.009	29.28	0.00730	0.00016	0.455	0.069
	1775.6	1.155	0.124	0.124	0.013	5.568	0.260	0.254	0.010	34.64	0.00864	0.00022	0.486	0.053
	890	1.112	0.120	0.119	0.012	4.633	0.217	0.207	0.012	53.17	0.01326	0.00026	0.573	0.065
	395.2	0.898	0.097	0.096	0.010	3.684	0.172	0.165	0.011	40.79	0.01018	0.00064	0.581	0.072
	247.4	0.923	0.099	0.099	0.016	3.302	0.154	0.147	0.011	40.00	0.00998	0.00022	0.669	0.120
	99.2	1.044	0.112	0.112	0.014	3.521	0.165	0.157	0.010	46.12	0.01151	0.00024	0.712	0.103
	29.5	0.963	0.103	0.103	0.017	2.250	0.105	0.100	0.009	30.23	0.00754	0.00017	1.032	0.194
	5.1	0.768	0.083	0.082	0.013	1.612	0.075	0.071	0.011	23.73	0.00592	0.00014	1.154	0.254
69	3676.5	0.404	0.043	0.043	0.006	2.031	0.095	0.092	0.013	19.60	0.00489	0.00014	0.471	0.093
55.84°N	3637.3	0.336	0.036	0.036	0.007	2.005	0.094	0.090	0.010	19.15	0.00478	0.00013	0.397	0.093
48.09°W	3589.5	0.438	0.047	0.047	0.007	2.234	0.104	0.101	0.011	21.39	0.00534	0.00014	0.465	0.086
	3444.7	0.528	0.057	0.056	0.007	3.666	0.171	0.167	0.012	27.76	0.00692	0.00016	0.339	0.047
	2951.8	0.581	0.062	0.062	0.007	5.835	0.273	0.267	0.014	33.80	0.00843	0.00019	0.232	0.029
	2462.6	0.604	0.065	0.064	0.007	6.523	0.305	0.298	0.013	39.48	0.00985	0.00021	0.216	0.024
	2168.1	0.855	0.092	0.091	0.007	6.120	0.286	0.279	0.013	40.95	0.01022	0.00023	0.327	0.030
	1481.3	0.670	0.072	0.071	0.006	5.068	0.237	0.223	0.012	79.22	0.01976	0.00038	0.318	0.032
	989	0.729	0.078	0.078	0.007	4.620	0.216	0.206	0.013	57.18	0.01427	0.00029	0.377	0.040
	445.6	0.692	0.074	0.074	0.005	4.312	0.202	0.192	0.014	55.48	0.01384	0.00028	0.384	0.037
	248.8	0.604	0.065	0.064	0.004	4.150	0.194	0.184	0.011	59.43	0.01483	0.00030	0.350	0.032
	99.5	0.513	0.055	0.054	0.006	3.664	0.171	0.162	0.014	56.06	0.01399	0.00029	0.337	0.046
	28.7	0.554	0.059	0.059	0.004	1.584	0.074	0.069	0.015	30.11	0.00751	0.00017	0.859	0.191
	8.2	0.457	0.049	0.049	0.004	1.503	0.070	0.064	0.010	34.28	0.00855	0.00018	0.757	0.140

Station	Depth	^{231}Pa	^{231}Pa	^{231}Pa$_{corr}$	2se	^{230}Th	^{230}Th	^{230}Th$_{corr}$	2se	^{232}Th	^{232}Th	2se	^{231}Pa/^{230}Th	2se
	m	fg/kg	dpm/1000l	dpm/1000		fg/kg	dpm/1000l	dpm/1000l		pg/kg	dpm/1000l			
77	2487.5					4.120	0.193	0.188	0.009	29.43	0.00734	0.00015		
53°N	2462.8	1.261	0.136	0.135	0.009	4.165	0.195	0.190	0.009	30.06	0.00750	0.00015	0.713	0.058
51.10°W	2414.2	1.113	0.120	0.119	0.006	4.190	0.196	0.191	0.009	29.56	0.00738	0.00015	0.625	0.043
	2268.5	0.989	0.106	0.106	0.007	6.228	0.291	0.285	0.010	33.99	0.00848	0.00018	0.371	0.029
	2170.5	1.355	0.146	0.145	0.008	5.412	0.253	0.248	0.010	30.77	0.00768	0.00016	0.586	0.040
	1678.1	1.267	0.136	0.136	0.008	5.577	0.261	0.254	0.010	37.02	0.00924	0.00018	0.533	0.038
	1235.4	0.580	0.062	0.062	0.008	5.483	0.256	0.249	0.011	44.75	0.01116	0.00022	0.249	0.034
	989.6	1.772	0.190	0.190	0.014	5.052	0.236	0.227	0.010	53.23	0.01328	0.00024	0.836	0.072
	496.4					4.427	0.207	0.197	0.010	55.68	0.01389	0.00026		
	297.9	0.501	0.054	0.053	0.004	4.802	0.225	0.213	0.014	64.41	0.01607	0.00032	0.249	0.025
	78.8	1.200	0.129	0.128	0.009	3.591	0.168	0.157	0.012	65.47	0.01633	0.00031	0.819	0.084
	2.5	0.926	0.100	0.099	0.007	1.434	0.067	0.062	0.011	28.01	0.00699	0.00015	1.595	0.295

^{230}Th and ^{231}Pa are dissolved ^{230}Th and ^{231}Pa activities corrected for the ingrowth from seawater ^{234}U and ^{235}U, respectively, since the time of collection following equations:

$$^{230}Th = {}^{230}Th_m - {}^{238}U \times (1 - \exp(-\lambda_{230Th} \times t)) \quad (1)$$

$$^{231}Pa = {}^{231}Pa_m - {}^{235}U \times (1 - \exp(-\lambda_{231Pa} \times t)) \quad (2)$$

^{230}Th and ^{231}Pa are further corrected for detrital, U-supported ^{230}Th and ^{231}Pa concentrations as follows:

$$^{230}Th_{\ corr} = {}^{230}Th_m - (0.7 \times {}^{232}Th_m) \quad (3)$$

$$^{231}Pa_{\ corr} = {}^{231}Pa_m - 0.046 \times (0.7 \times {}^{232}Th_m) \quad (4)$$

where $^{230}Th_m$, $^{231}Pa_m$ and $^{232}Th_m$ are activities obtained from measurement; ^{235}U and ^{238}U are their average activities in seawater, 118 dpm/1000l and 2436 dpm/1000l, respectively; λ_{230Th} and λ_{231Pa} are decay constants of ^{230}Th and ^{231}Pa; t is the time between sample collection and chemical separation of U from ^{231}Pa and ^{230}Th. 0.7 is the average ^{238}U/^{232}Th activity ratio in detrital material (Marcantonio et al., 2001) and 0.046 represents the ^{235}U/^{238}U activity (Anderson et al., 1990). Activities of ^{231}Pa, ^{230}Th and ^{232}Th have been converted to dpm/1000l assuming the density of seawater ρ= 1.025g/cm^3. Half-lives for ^{231}Pa, ^{230}Th and ^{232}Th are 32,760 yr, 75,584 yr and 1.40×10^{10} yr (Robert et al., 1969; Cheng et al., 2013; Holden, 1990).

All errors are two standard errors including the contribution from sample weighing, spike calibration, ^{231}Pa, ^{230}Th and ^{232}Th in the respective ^{233}Pa and ^{230}Th spikes, blank correction, internal precision and related corrections of mass spectrometric measurement.

S2. CFC-based Age determination

CFC measurement are not available along the GEOVIDE line. However, Paz et al. (2017) determined the CFC-based age along the same line in 2012 (OVIDE/CATARINA cruise). We projected the CFC-based age along GEOVIDE line using the water mass distributions (Steinfeldt personal communication) along GEOVIDE line given by Garcia-Ibanez et al. (2018) and the distribution for the same water masses in 2012 (García-Ibáñez et al., 2015). The water mass analysis was applied already for different purposes related with the chemical characterization. This approach was successfully applied to dissolved-organic-carbon water mass definitions in the North Atlantic (Fontela et al., 2016) and for evaluating the impact of water mass mixing and remineralization on the N_2O distribution in the North Atlantic (Paz et al., 2017). Previous studies have also applied the water mass analysis to determine the nutrient ratio utilization and organic matter mineralization (Pérez et al., 1994, Brea et al., 2004; Álvarez-Salgado et al., 2013). Cossa et al. (2018) characterized the HgT_{UNF} concentration of each water mass using the water mass analysis shown here. The first step determined the CFC-age for each Source Water Types (SWTs) defined in García-Ibáñez et al. (2015). They have used an extended Optimum Multi-Parameter (eOMP) analysis to quantifies the fractions of the different Source Water Types (SWTs) that contribute to a given water sample for OVIDE line done in 2012. The CFC-age for each SWT *"i"* (12 unknowns $[\text{CFC-age}]_i$) were estimated through an inversion of the following systems of 424 equations:

$$\log\,[\text{CFC} - \text{Age}]^j = \sum_{i=1}^{12} SWT_i^j \times (\log[\text{CFC} - \text{Age}]_i) + \varepsilon_j \; j = 1 \rightarrow 424\; samples \quad (5)$$

where SWT_i^j are the fractions of SWT *"i"* to sample *"j"* (obtained through the eOMP analysis), $[CFC\text{-}age]^j$ is the CFC-age for each sample measured in 2012, and ε_j the residual. The 424 ε_js of the inversion resented a null mean and a standard deviation of 0.12 (R^2 = 0.94). The output of the inversion ($[\text{CFC-age}]_i$) is given in Table S2. With this output, we use the same equation to compute the [CFC-age] of each water sample of GEOVIDE cruise, using the fractions of the each SWT obtained by Garcia-Ibañez et al. (2018) for GEOVIDE. Because of the low fractions of the SWT $SAIW_4$, its fraction has been added to $SAIW_6$.

Table S2 The output of the inversion $[\text{CFC-age}]_i$

	log(CFC-age)	CFC-age
$ENACW_{16}$	1.05±0.20	11±5
$ENACW_{12}$	1.11±0.03	13±1
$SPMW_8$	1.69±0.04	49±5
SAIW	1.19±0.07	16±3
$SPMW_7$	1.26±0.05	18±2
IrSPMW	0.98±0.03	10±1
LSW	1.54±0.02	35±1
MW	1.96±0.04	91±8
PIW	1.33±0.15	22±8
DSOW	1.22±0.07	17±3
ISOW	1.70±0.03	50±4
$NEADW_L$	3.00±0.02	989±48
r^2	0.94	0.943
std(Resid)	0.12	41

S3. Scavenging-mixing model and parameterization

A more detailed description of the scavenging-mixing model this study adapted from is given in Moran et al. (1997). Briefly, the model takes into account reversible scavenging of the nuclides and water mass mixing. It describes the evolution of nuclides through time of a one-dimensional system, an ocean water column. In the Atlantic, the system is assumed to start at time t=0 in the far North Atlantic and moves southward with time. Transport of material downward relative to the direction of water flow is permitted, to represent the effect of scavenging of radionuclides by sinking particles. Lateral exchange with water outside of the 1-D system is not permitted.

The equation to derive the dissolved concentration of each nuclide follows that of Moran et al., (1997). From observation, however, the concentration of ^{230}Th and ^{231}Pa are in most of cases not 0 at the surface (i.e. z=0). We therefore introduce a surface term to reflect this observation and set its value the same as the preformed concentration. Dissolved concentration of the nuclide can be then derived with the equation:

$$c_d = \frac{C_{pre} + P \quad T_w}{(K_d\ SPM+1)} \times [1 - \exp(\frac{-z(K_d\ SPM+1)}{SK_d\ T_w\ SPM})] + C_{surface} \quad (6)$$

where C_d is the dissolved concentration of the nuclide ; P is the production rate of ^{230}Th and ^{231}Pa, 2.57 × 10^{-2} dpm/1000l/yr and 2.37 × 10^{-3} dpm/1000l/yr, respectively; K_d is the distribution coefficient of the nuclide; λ is the decay constant of the nuclide; C_{pre} is the preformed concentration of ^{230}Th (or ^{231}Pa); $C_{surface}$ is the concentration of ^{230}Th and ^{231}Pa in surface water, set at a value the same as the preformed concentration for both nuclides; SPM is the suspended particle concentration; and S is the particle settling speed, which represents the net effect of particle sinking, disaggregation and aggregation; T_w is water mass age; z is the water depth.

Initial parameterization was conducted using S=500-1000 m/yr, K_d^{Th}= 1× 10^7 ml/g, K_d^{Pa}= 5× 10^5 ml/g, SPM= 20-50 µg/l, for preformed concentrations set at 0 and surface average from GEOVIDE, i.e., $C_{pre}^{Th} = C_{surface}^{Th}$ = 0.108 dpm/1000l, C_{pre}^{Pa}=$C_{surface}^{Pa}$= 0.089 dpm/1000l. With T_w known from CFC measurements for every depth where ^{230}Th and ^{231}Pa was measured along GEOVIDE section, water-column profiles of both nuclides were simulated for GEOVIDE station 1 and 13 and the parameters were adjusted for the best fit between the simulated and observed profiles (Fig. S1). This gives us the optimised parameters for the analysis in discussion section 4.3, which are listed in Table S3. Our optimized parameters are consistent with values reported by other studies (also listed in Table S3).

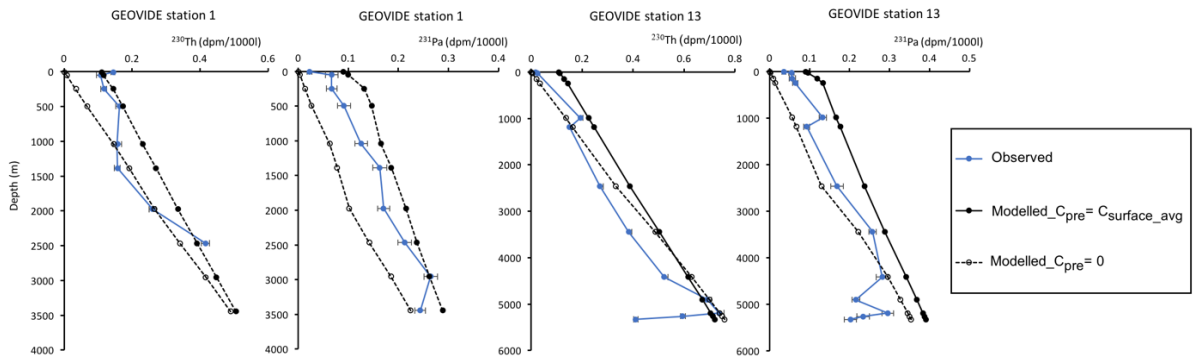

Figure S1: Modelled (dashed black lines) profiles with preformed value set at 0 and surface average concentration from GEOVIDE, and observed (solid blue lines) profiles of station 1 and 13 from GEOVIDE section. The best fit was first sought for ^{230}Th, which gives us the optimized parameters S, SPM and K_d^{Th}. These parameters were then adopted for the simulation of ^{231}Pa profiles, adjusting only K_d^{Pa} to obtain the best fit.

Table S3 Parameterization of the scavenging-mixing model

	This study	Literature
S (m/yr)	800	500-1000 (Moran et al., 1997)
SPM (µg/l)	25	30 (Labrador Sea, Brewer et al., 1976)
K_d^{Th} (ml/g)	1.1×10^7	1.1×10^7 (Moran et al., 1997)
K_d^{Pa} (ml/g)	2×10^6	2.2×10^5 (pure carbonate)~1.4×10^6 g/g (pure opal) (pseudo-K_d, Chase et al., 2002)

Additional references

Álvarez-Salgado, X. A., M. Nieto-Cid, M. Álvarez, F. F. Pérez, P. Morin, and H. Mercier: New insights on the mineralization of dissolved organic matter in central, intermediate, and deep water masses of the northeast North Atlantic, *Limnol Ocean.*, *58*(2), 681–696, doi:10.4319/lo.2013.58.2.0681, 2013.

Anderson, R.F., Lao, Y., Broecker, W.S., Trumbore, S. and J. Hofmann, H.: Boundary scavenging in the Pacific Ocean - A comparison of Be-10 and Pa-231., 1990.

Brea, S., X. A. Álvarez-Salgado, M. Álvarez, F. F. Pérez, L. Mémery, H. Mercier, and M. J. Messias: Nutrient mineralization rates and ratios in the eastern South Atlantic, *J. Geophys. Res.*, *109*, C05030, doi:10.1029/2003JC002051, 2014.

Brewer, P. G., Spencer, D. W., Biscaye, P. E., Hanley, A., Sachs, P. L., Smith, C. L., Kadar, S. and Fredericks, J.: The distribution of particulate matter in the Atlantic Ocean, Earth Planet. Sci. Lett., 32(2), 393–402, doi:https://doi.org/10.1016/0012-821X(76)90080-7, 1976.

Chase, Z., Anderson, R. F., Fleisher, M. Q. and Kubik, P. W.: The influence of particle composition and particle flux on scavenging of Th, Pa and Be in the ocean, Earth Planet. Sci. Lett., 204(1), 215–229, doi:https://doi.org/10.1016/S0012-821X(02)00984-6, 2002.

Cossa D., L-E Heimbürger, F. F. Pérez, M. I. García-Ibáñez, J. E. Sonke, H. Planquette, P. Lherminier, G. Sarthou: Mercury distribution and transport 1 in the North Atlantic Ocean along the GEOTRACES-GA01 transect. Biogeosciences https://doi.org/10.5194/bg-2017-467, 2018.

Fontela, M., M. I. García-Ibáñez, D. A. Hansell, H. Mercier, and F. F. Pérez: Dissolved organic carbon in the North Atlantic meridional overturning circulation, *Sci. Rep.*, *6*, 26931, doi:10.1038/srep26931, 2016.

Marcantonio, F., Anderson, R. F., Higgins, S., Fleisher, M. Q., Stute, M. and Schlosser, P.: Abrupt intensification of the SW Indian Ocean monsoon during the last deglaciation: constraints from Th, Pa, and He isotopes, Earth Planet. Sci. Lett., 184(2), 505–514, doi:https://doi.org/10.1016/S0012-821X(00)00342-3, 2001.

Pérez, F. F., C. Mouriño, F. Fraga, and A. F. Rios: Displacement of water masses and remineralization rates off the Iberian Peninsula by nutrient anomalies, *J. Mar. Res.*, *51*, 869–892, doi:10.1357/0022240933223891, 1993.

Reinthaler, T., X. A. Álvarez Salgado, M. Álvarez, H. M. van Aken, and G. J. Herndl: Impact of water mass mixing on the biogeochemistry and microbiology of the Northeast Atlantic Deep Water, *Glob. Biogeochem. Cycles*, *27*(4), 1151–1162, doi:10.1002/2013GB004634, 2013.